electron properties and hence will have a bearing on the calculated dipole moment components. Fig. 6 shows the experimental Laplacian $\nabla^2\rho_b(\mathbf{r})$, which clearly shows the features of all the intramolecular interactions. At the end of the refinement the P_v value of the S atom is 5.29 (4) while that of the O atom is 6.28 (4), and these values depict the nature of the charge distribution in the valence shell in this molecule. The refined κ-parameters show a contraction of the S atom ($\kappa = 1.16$) while the O atom remains intact ($\kappa = 1.00$). However, all C atoms show a slight contraction ($\kappa = 1.03$). The corresponding κ' values are 0.85 for S, 0.96 for O and 0.88 for C atoms.

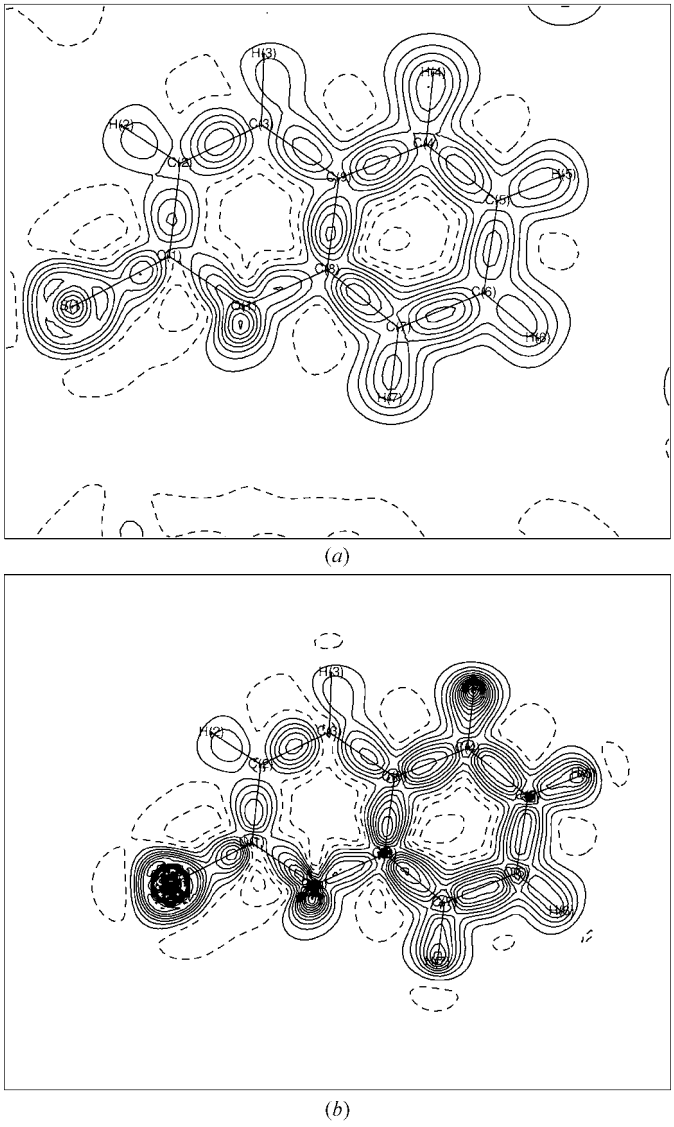

Figure 4
(*a*) Dynamic-deformation density map in the plane of the molecule. The first positive contour is at 0.05 e Å^{-3} and the contour levels are at 0.1 e Å^{-3} intervals. The first negative contour is at −0.05 e Å^{-3} and the contour levels are at −0.1 e Å^{-3} intervals. The solid lines are positive contours and the broken lines are negative contours. (*b*) Static-deformation density map in the plane of the molecule. The positive contour levels are at 0.1 e Å^{-3} intervals and the negative contour levels are at −0.1 e Å^{-3} intervals. The solid lines are positive contours and the broken lines are negative contours.

Table 3
Intramolecular bond critical points and their properties.

Bond	$\rho_b(\mathbf{r})$	$\nabla^2\rho_b(\mathbf{r})$	$D1$	$D2$	λ_1	λ_2	λ_3	ε
S(1)−C(1)	1.558	−3.264	0.8215	0.8340	−10.16	−8.06	14.95	0.26
O(1)−C(8)	2.112	−19.235	0.8193	0.5574	−18.58	−16.55	15.90	0.12
O(1)−C(1)	1.995	−18.421	0.8504	0.5137	−17.13	−15.43	14.13	0.11
C(8)−C(9)	2.150	−20.449	0.7335	0.6652	−17.82	−13.63	11.00	0.31
C(8)−C(7)	2.198	−20.085	0.7336	0.6615	−17.41	−13.99	11.32	0.24
C(3)−C(9)	2.020	−15.567	0.7060	0.7288	−15.31	−12.70	12.45	0.21
C(3)−C(2)	2.490	−25.702	0.7191	0.6402	−20.28	−16.36	10.94	0.24
C(9)−C(4)	2.213	−19.265	0.7231	0.6882	−17.14	−14.14	12.02	0.21
C(2)−C(1)	1.954	−15.685	0.6852	0.7507	−14.86	−12.37	11.54	0.20
C(4)−C(5)	2.150	−19.134	0.7019	0.6844	−17.07	−13.63	11.57	0.25
C(7)−C(6)	2.324	−17.907	0.6862	0.7056	−17.36	−13.83	13.29	0.26
C(6)−C(5)	2.073	−15.821	0.7031	0.7024	−15.59	−12.78	12.55	0.22

Since our main aim is to obtain an accurate molecular dipole moment, the program *XDPROP* from the *XD* package is employed to obtain the components of the dipole moment. Table 4 gives the values of the components and the value of the net dipole moment that are obtained from the experiment. Table 4 also provides the values for the dipole moments as obtained from theoretical calculations based on the package *GAUSSIAN*98. The calculations have been performed using both HF and DFT methods. The DFT method (basis set 6-311G**) produces a dipole moment that is significantly smaller than that obtained using the *ab initio* HF method at the same level. The molecular geometry as found in the final refinement has been adopted in all the calculations. In the charge-density analysis of a polar molecule, 2-methyl-4-nitroaniline (Howard *et al.*, 1992), it is observed that the experimentally determined value of the dipole moment is rather high compared with the theoretically determined value. A similar feature is also observed in the structure of 2-thiocoumarin. The main contributors to the dipole-moment components are the S and the O atoms in this structure. The coordinates and the population parameters of the valence shell P_v, and their corresponding values of P_{11+}, P_{10}, P_{11-} and

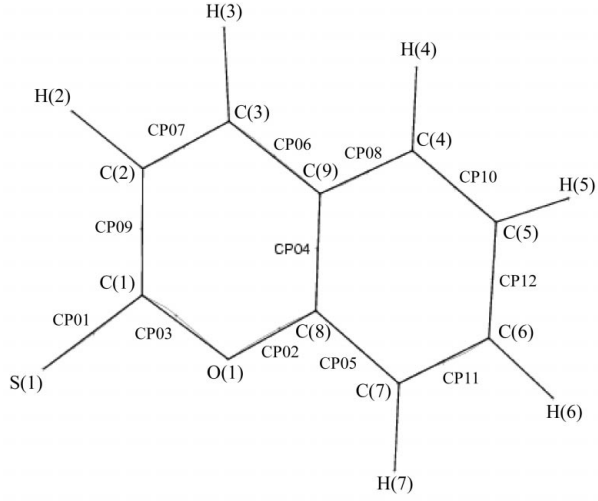

Figure 5
Bond-path character in the molecule showing the critical-point locations along the bonds.